Non-Contact Acoustic Emission Monitoring of Corrosion-Fatigue Damage in Submerged Steel Structures

FILIPPO RICCIOLI and LOTFOLLAH PAHLAVAN

ABSTRACT

Corrosion-fatigue is considered one of the main degradation mechanisms affecting the structural integrity of offshore support structures and mooring systems. These structures are typically covered with marine growth of various types. This paper highlights a feasibility assessment of detection and localization of corrosion-fatigue damage in submerged steel structures using non-contact Acoustic Emission (AE) technique. An accelerated corrosion-fatigue experiment was conducted on a dog-bone steel specimen. A dedicated experimental set-up was designed to simultaneously apply accelerated corrosion and cyclic loading on the dog-bone steel specimen submerged in artificial seawater. Ultrasound signals were continuously measured using an array of underwater AE transducers (in the frequency range between 50-450 kHz) placed at a fixed distance from the tested coupon. A source localization algorithm for corrosion-fatigue-induced ultrasound signals was successfully implemented. The results of the accelerated corrosion-fatigue experiment suggest that corrosion-fatigue-induced ultrasound signals can be detected with a satisfactory signal-to-noise ratio using non-contact AE transducers. Four stages of corrosion-fatigue damage growth were identified which may be used as the basis for possible damage characterization.

INTRODUCTION

Corrosion-fatigue is regarded as one of the main degradation mechanisms of offshore support structures, and mooring systems [1-5]. Structural integrity assessment of the submerged part of these structures can be challenging due to difficult access, waves, and weather conditions, etc. Additionally, the presence of marine growth on the surface of the submerged structure often requires the need of surface cleaning to obtain a detailed assessment of the structural integrity. This process is highly undesirable from technical, economical, end environmental points of view.

Acoustic Emission (AE), a passive ultrasound method, is an established monitoring technique for assessment of different types of damage [6-12]. AE technique can enable

Filippo Riccioli, Delft University of Technology, 2628 CD Delft, The Netherlands Lotfollah Pahlavan, Delft University of Technology, 2628 CD Delft, The Netherlands

the identification, localization, and characterization of corrosion-fatigue damage by continuously monitoring the transient stress waves generated by the rapid release of energy from localized sources within the material. Every localized AE event can be related to the onset of new damage or to the progression of an active fault in the material structure. The corrosion-fatigue-induced AE sources can be characterized by their specific properties [13]. Significant and highly energetic sources of AE can be identified in crack initiation and growth [13-18], as well as in the breakdown of thick oxide films (in high-temperature water) [13]. Despite being associated with a lower energy level, the evolution of hydrogen gas (due to cathodic reaction in acid solutions) is also considered a primary source of AE in the corrosion-fatigue process [13; 19-22]. Possible secondary sources of AE in the corrosion-fatigue process include transformation, deformation, fracture of precipitates, and micro-cracking in the crack tip plastic zone [13-15; 21-25]. These mechanisms are typically associated with a medium AE energy level [13]. While the dissolution of metal or breakdown of thin passive film is also considered a potential source of AE, the energy level associated with it is believed to be too small to detect [13]. Limited investigations on the detection and monitoring of ultrasound signals using non-contact AE technique have also been reported in the literature [26-29]. Recently, the authors have investigated the detectability of AE signals during accelerated corrosion process using non-contact AE transducers [7].

Acoustic Emission is a valuable technique for detecting, localizing, and monitoring corrosion-fatigue damage.

This paper investigates the feasibility of detection and localization of corrosion-fatigue damage in submerged steel structures using non-contact AE measurements. Accelerated corrosion-fatigue experiments have been performed on a dog-bone steel specimen to detect and localize corrosion-fatigue-induced AE using an array of underwater AE transducers. A source localization algorithm for the induced ultrasound signals has been implemented, and the results verified with the observed damage. Four stages of corrosion-fatigue damage growth have been identified using the AE hit-rate and the cumulative number of localized AE signals.

The paper has the following structure. The methodology is presented in Section 2. Description of the experiment is given in Section 3. The results are presented and discussed in Section 4, followed by the conclusions in Section 5

METHODOLOGY

For a submerged steel specimen subject to corrosion-fatigue, Figure 1 schematically shows the ultrasound wave propagation with a non-contact AE transducer.

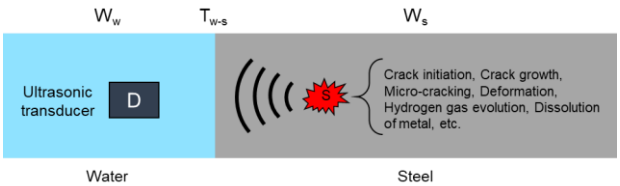

Figure 1. Schematic illustration of the wave propagation path in submerged steel specimen with a non-contact AE transducer.

Damage-induced ultrasound waves, denoted by source S, can propagate through the steel medium as bulk waves (i.e. longitudinal and shear mode), surface (i.e. Rayleigh) waves, or guided waves depending on the frequency of the waves and the thickness of the medium [30]. Ultrasound waves can further propagate through the water medium as pressure waves (constant speed of sound). Wave components with sufficient energy (to overcome geometrical spreading and material attenuation) can reach the ultrasound transducer. The measured signals P can be described in the frequency domain as the convolution of the source signal S with the transfer functions of the media and interfaces involved in the wave path, as in

$$P = DW_w T_{w-s} W_s S + N \tag{1}$$

where W_s and W_w are the propagation (transfer) functions of steel and water respectively. $T_{w\text{-}s}$ is the transmission coefficient between steel and water, and D is the transfer function of the sensor. N refers to the background noise and the neglected components of the wave.

Acoustic Emission (AE) Monitoring of Corrosion-Fatigue Damage

The variation of the AE hit-rate (i.e. rate of burst-type signals per loading cycle) is used to detect and monitor active AE sources. Every relevant AE event can indicate the onset of new damage or the propagation of an active defect in the material structure. The variation in the rate of AE may provide insight into the rate of damage growth. Additionally, the evolution of the cumulative number of localized burst-type signals enables the assessment of the corrosion-fatigue-induced damage evolution. Different stages of damage growth have been identified and distinguished in various testing conditions such as corrosion, fatigue, and corrosion-fatigue [15-18; 24; 31].

EXPERIMENTS

A dedicated experimental set-up was designed to simultaneously apply accelerated corrosion and fatigue loading on a steel specimen submerged in artificial seawater. Figure 2 (left) shows a schematic illustration of the corrosion-fatigue experimental set-up and equipment.

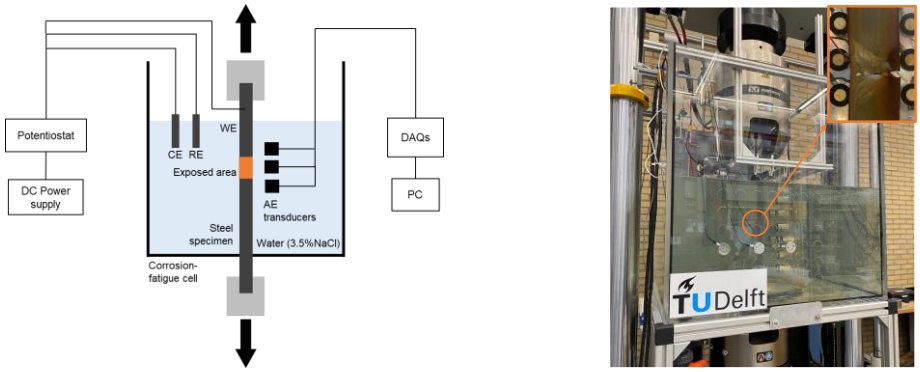

Figure 2. Schematic illustration of the corrosion-fatigue test set-up (left), and corrosion-fatigue experimental set-up and dog-bone steel specimen after failure (right).

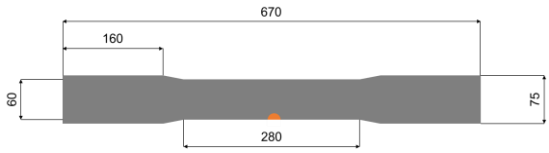

Figure 3. Schematic representation of the dog-bone specimen with the exposed (orange) area. Dimensions in mm.

Figure 2 (right) shows the corrosion-fatigue cell. An aluminum support frame was used to accommodate the 630x630x630mm^3 Plexiglas tank between the two grips of the fatigue testing machine. Figure 3 shows a schematic representation of the dog-bone specimen along with its dimensions. The overall length and width of the steel specimen are 670 mm and 75 mm, respectively. The gauge area extends for 280 mm in length and 60 mm in width.

The chosen material for the dog-bone specimen, i.e. S420NL, is characterized by a yield stress of 420 N/mm^2, a tensile strength of 480-620 N/mm^2, and an elongation of 20%. The mechanical properties of the selected material are in the range of those characteristic of R3 steel grade (a typical steel grade for offshore support structures and mooring chains). The corrosion-fatigue damage was induced in the exposed (to artificial seawater) area of the dog-bone specimen (Figure 3). The exposed surface is a half-circle (about 20 mm in diameter) located at the edge of the width of the specimen in line with the center of the gauge area.

Accelerated corrosion-fatigue process

An Instron axial-torsion servo-hydraulic testing machine (Figure 2) was used to apply a uniaxial fatigue load on the tested coupon. The specimen was subject to sinusoidal cyclic load with a maximum peak load of 168 kN, load ratio of 0.18, and loading frequency of 2 Hz. A three-electrodes potentiostatic system was employed to control the accelerated corrosion process. A working electrode (i.e. exposed surface), a counter electrode (i.e. graphene bar), and a reference electrode (i.e. Ag/AgCl electrode) compose the three-electrodes system in artificial seawater. A fixed concentration of NaCl (equal to 3.5%) was used. A stable electrochemical potential (equal to −0.435 V) was set to maintain a fixed corrosion rate at the exposed steel surface.

The specimen was subject to an accelerated corrosion process for about 100 hours prior to testing. This process was used to simulate the initiation of surface defects and referred to as ‘pre-corrosion’.

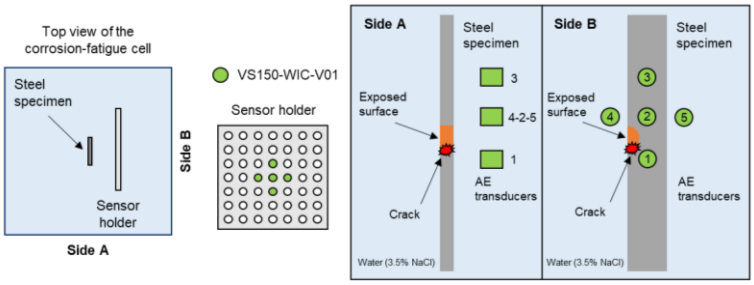

Figure 4. Schematic illustration of the layout of the AE transducers.

Data acquisition, management, and quality control

To collect and record the ultrasound signals generated during the corrosion-fatigue process an AMSY-6 Vallen data acquisition (DAQ) system and five watertight piezoelectric AE transducers (VS150-WIC-V01, with an integrated preamplifier, gain of 34 dB) were employed [32]. Watertight co-axial cables connected the piezoelectric AE transducers to the DAQ system. Figure 4 schematically shows the layout of the AE transducers. A fixed distance (equal to 70 mm) was kept between the specimen and the AE transducers using a sensor holder (400x400mm^2 acrylic plate with 7x7 grid of holes 50 mm equispaced). A sampling rate of 2,5 MHz was used to record the AE signal waveforms (with a total sample length of 4.096 points).

Pencil lead break tests (according to ASTM E976-15 [33]) in the area of the exposed surface were performed to check the proper functioning of the AE measurement system and to verify the localization algorithm prior to testing.

For the noise level assessment, a dummy dog-bone steel specimen was subject to cyclic loading in artificial seawater for about 1 hour. The maximum measured noise level was about 50 dB. The acquisition threshold was set to 50 dB.

The recorded ultrasound signals have been pre-processed using a filter based on signal-to-noise ratio (SNR) value of 2 to separate potential damage-induced signals from the background noise (i.e. continuous-type signals). An AE source localization algorithm, based on triangulation technique [34] has been implemented.

RESULTS AND DISCUSSION

Experiments described in Section 3 were performed and the methodology for the data analysis described in Section 2 was applied.

Figure 5 shows the variation of the AE hit-rate and the evolution of the normalized cumulative number of AE signals as a function of the normalized number of load cycles. Four time periods (labeled A to D) are identified and distinguished by black dash-dot lines. The four time periods can be related to different stages of corrosion-fatigue-induced damage growth. During Stage A, the AE hit-rate is high, possibly indicating the initiation of crack formation. Stage B is characterized by a lower AE hit-rate (than the previous stage). The AE hit-rate remains stable at around 1 burst-type signal per cycle, as detected by the most sensitive transducers. This may indicate a stable crack growth with a low rate of propagation. In Stage C, the AE hit-rate suddenly increases, settling at a stable level of approximately 2.5 burst-type signals per cycle. This may suggest a stable crack growth at a higher rate. Stage D is characterized by a low AE hit-rate, followed by a sudden increase close to the specimen final failure. This may be related to unstable crack growth.

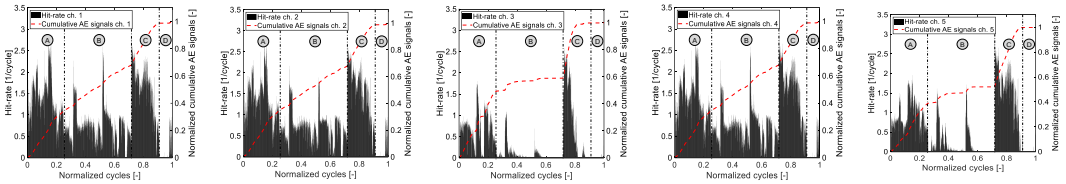

Figure 5. Variation of AE hit-rate and evolution of the normalized cumulative number of AE signals as a function of the normalized number of load cycles. Channels 1-5 are shown from left to right.

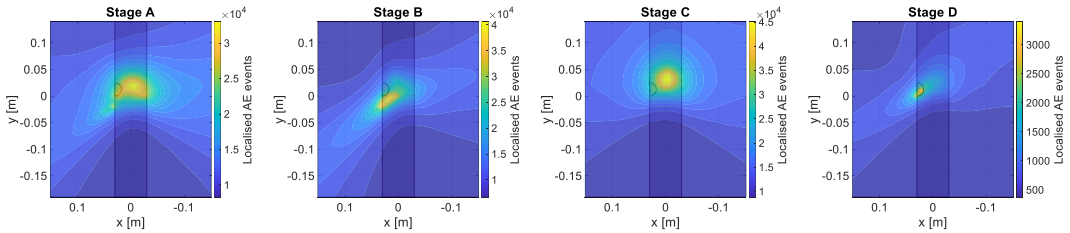

Figure 6. Localization map for different stages of the corrosion-fatigue damage evolution.

During Stage A, the cumulative number of AE signals increases rapidly, followed by a slower rate of increase during Stage B. However, Stage C exhibits a sudden and rapid rise in the cumulative values, resulting in a steep curve that is similar to Stage A. Despite the growth rate of the number of AE signals gradually decreases towards the end of Stage C, the cumulative value experiences a sharp increase near the end of Stage D as a result of the final fracture. It should be noted that different secondary effects, that may contribute to the spiked variations of the AE hit-rate, are mitigated in the cumulative number of AE signals. Nonetheless, it appears that the cumulative number of AE signals offers promising indications about the stages of damage growth, emphasizing the feasibility of detection and monitoring of corrosion-fatigue-induced ultrasound using non-contact AE transducers.

The AE source localization map for the four stages of the corrosion-fatigue damage growth has been calculated by summation of the normalized inverse error matrix (calculated over the grid points for each localized event). The grid has uniform spacing of 10 mm in both x and y directions. A maximum allowable error value of 15 μs has been used. Figure 6 shows the localization map for the four stages of the corrosion-fatigue damage evolution. In Stage A, the localized AE events are distributed in the center of the specimen and extend to the bottom edge of the exposed surface (where the corrosion-fatigue damage developed). The maximum number of AE events seems to be about 20 mm distant from the exposed surface, while a high number of AE events (in the order of $3x10^4$) are localized at the bottom edge of the exposed area. During Stage B, the maximum number of AE events (in the order of $4x10^4$) is localized near the bottom edge of the exposed surface. This slight shift (about 10-20 mm) could be due to the choice of the time-picking algorithm. Improvements can be made in the future work. In Stage C, the maximum number of events seems to be located in the center of the specimen, i.e. 20-30 mm from the crack location. The results of the localization may be explained by the combined effect of damage growth and time-picking error, however limited. Stage D mostly shows AE events induced by the final fracture. The maximum number of localized events seems to be focused in a narrow area that overlays the position of the induced crack.

CONCLUSIONS

Feasibility of monitoring corrosion-fatigue damage in submerged steel structures using the non-contact AE technique was experimentally investigated. A dog-bone S420NL steel specimen was subject to accelerated corrosion-fatigue to detect and localize corrosion-fatigue-induced ultrasound using an array of underwater AE transducers. The corrosion-fatigue-induced ultrasound signals were detected with a

satisfactory signal-to-noise ratio. A source localization algorithm for corrosion-fatigue-induced ultrasound was successfully implemented, and the results were confirmed by the observed damage. AE sources were localized with an accuracy of about 20 mm.

Using the AE hit-rate and the cumulative number of localized AE signals, it was possible to distinguish four stages of corrosion-fatigue damage growth. During initiation of crack formation, an AE hit-rate of 2-2.5 signals per cycle was observed. Stable crack growth was associated with an AE hit-rate level of 1-2 and 1.5-2.5 signals per cycle for low and high rates of propagation respectively. The final failure of the specimen resulted in a measured AE hit-rate of 0.5-1 signals per cycle. This result can serve as the basis for future possible damage characterization using non-contact AE technique.

ACKNOWLEDGMENTS

This research has been conducted within the framework of DONUT Joint Industry Project (JIP). The project partners are acknowledged for their support and contribution. DONUT JIP has been made possible by the financial contribution of TKI Maritime. The authors are grateful to Sarjoon Alkhateeb for the design and fabrication of the corrosion-fatigue experimental setup.

REFERENCES

1. Adedipe, O., Brennan, F., & Kolios, A. (2016). Review of corrosion fatigue in offshore structures: Present status and challenges in the offshore wind sector. Renewable and Sustainable Energy Reviews, 61, 141-154.
2. Fontaine, E., Rosen, J., Potts, A., Ma, K. T., & Melchers, R. (2014, May). Scorch jip-feedback on MIC and pitting corrosion from field recovered mooring chain links. In Offshore technology conference. OnePetro.
3. Ma, K. T., Shu, H., Smedley, P., L'Hostis, D., & Duggal, A. (2013, May). A historical review on integrity issues of permanent mooring systems. In Offshore technology conference. OnePetro.
4. Melchers, R. E., Jeffrey, R., & Fontaine, E. (2012, July). Corrosion and the structural safety of FPSO mooring systems in Tropical waters. In Proceedings of the Australasian Structural Engineering Conference, Perth, WA, Australia (pp. 11-13).
5. Fontaine, E., Kilner, A., Carra, C., Washington, D., Ma, K. T., Phadke, A., ... & Kusinski, G. (2014, May). Industry survey of past failures, pre-emptive replacements and reported degradations for mooring systems of floating production units. In Offshore technology conference. OnePetro.
6. Calabrese, L., & Proverbio, E. (2020). A review on the applications of acoustic emission technique in the study of stress corrosion cracking. Corrosion and Materials Degradation, 2(1), 1-30.
7. Alkhateeb, S., Riccioli, F., Morales, F. L., & Pahlavan, L. (2022). Non-Contact Acoustic Emission Monitoring of Corrosion under Marine Growth. Sensors, 23(1), 161.
8. Scheeren, B., Kaminski, M. L., & Pahlavan, L. (2022). Evaluation of ultrasonic stress wave transmission in cylindrical roller bearings for acoustic emission condition monitoring. Sensors, 22(4), 1500.
9. Huijer, A., Kassapoglou, C., & Pahlavan, L. (2021). Acoustic emission monitoring of carbon fibre reinforced composites with embedded sensors for in-situ damage identification. Sensors, 21(20), 6926.
10. Van Steen, C., Pahlavan, L., Wevers, M., & Verstrynge, E. (2019). Localisation and characterisation of corrosion damage in reinforced concrete by means of acoustic emission and X-ray computed tomography. Construction and Building Materials, 197, 21-29.
11. Scheeren, B., Kaminski, M. L., & Pahlavan, L. (2023). Acoustic emission monitoring of naturally developed damage in large-scale low-speed roller bearings. Structural Health Monitoring, 14759217231164912.

12. Pahlavan, P. L., Paulissen, J., Pijpers, R., Hakkesteegt, H., & Jansen, R. (2014, July). Acoustic emission health monitoring of steel bridges. In EWSHM-7th European Workshop on Structural Health Monitoring.
13. Yuyama, S., Hisamatsu, Y., & Kishi, T. (1984). Fundamental aspects of AE monitoring on corrosion fatigue processes in austenitic stainless steel. J. Mater. Energy Syst.;(United States), 5(4).
14. Chang, H. (2014). Acoustic emission study of corrosion fatigue crack propagation mechanism identification. In Applied Mechanics and Materials (Vol. 628, pp. 20-23). Trans Tech Publications Ltd.
15. Chai, M., Zhang, J., Zhang, Z., Duan, Q., & Cheng, G. (2017). Acoustic emission studies for characterization of fatigue crack growth in 316LN stainless steel and welds. Applied acoustics, 126, 101-113.
16. Chai, M., Hou, X., Zhang, Z., & Duan, Q. (2022). Identification and prediction of fatigue crack growth under different stress ratios using acoustic emission data. International Journal of Fatigue, 160, 106860.
17. Chai, M., Lai, C., Xu, W., Duan, Q., Zhang, Z., & Song, Y. (2022). Characterization of Fatigue Crack Growth Based on Acoustic Emission Multi-Parameter Analysis. Materials, 15(19), 6665.
18. Calabrese, L., Bonaccorsi, L., Galeano, M., Proverbio, E., Di Pietro, D., & Cappuccini, F. (2015). Identification of damage evolution during SCC on 17-4 PH stainless steel by combining electrochemical noise and acoustic emission techniques. Corrosion Science, 98, 573-584.
19. Du, G., Li, J., Wang, W. K., Jiang, C., & Song, S. Z. (2011). Detection and characterization of stress-corrosion cracking on 304 stainless steel by electrochemical noise and acoustic emission techniques. Corrosion Science, 53(9), 2918-2926.
20. Fregonese, M., Idrissi, H., Mazille, H., Renaud, L., & Cetre, Y. (2001). Initiation and propagation steps in pitting corrosion of austenitic stainless steels: monitoring by acoustic emission. Corrosion science, 43(4), 627-641.
21. Ferrer, F., Faure, T., Goudiakas, J., & Andrès, E. (2002). Acoustic emission study of active–passive transitions during carbon steel erosion–corrosion in concentrated sulfuric acid. Corrosion Science, 44(7), 1529-1540.
22. Jirarungsatian, C., & Prateepasen, A. (2010). Pitting and uniform corrosion source recognition using acoustic emission parameters. Corrosion Science, 52(1), 187-197.
23. Chang, H., Han, E., Wang, J. Q., & Ke, W. (2005). Acoustic emission study of corrosion fatigue crack propagation mechanism for LY12CZ and 7075-T6 aluminum alloys. Journal of materials science, 40, 5669-5674.
24. Han, Z., Luo, H., Cao, J., & Wang, H. (2011). Acoustic emission during fatigue crack propagation in a micro-alloyed steel and welds. Materials Science and Engineering: A, 528(25-26), 7751-7756.
25. Chang, H. (2015). Identification of damage mode in AZ31 magnesium alloy under tension using acoustic emission. Transactions of Nonferrous Metals Society of China, 25(6), 1840-1846.
26. Sutowski, P., Nadolny, K., & Kaplonek, W. (2012). Monitoring of cylindrical grinding processes by use of a non-contact AE system. International Journal of Precision Engineering and Manufacturing, 13, 1737-1743.
27. Schmidt, P. L., Nelson, J. K., Handy, R. G., Morrell, J. S., Jackson, M. J., & Rees, T. M. (2017). Noncontact measurements of acoustic emissions from the single-point turning process. The International Journal of Advanced Manufacturing Technology, 93, 3907-3920.
28. Matsuo, T., & Hatanaka, D. (2019). Development of non-contact fatigue crack propagation monitoring method using air-coupled acoustic emission system. Engineering Transactions, 67(2), 185-198.
29. Xiao, W., & Yu, L. (2021, March). Non-contact passive sensing of acoustic emission signal using the air-coupled transducer. In Health Monitoring of Structural and Biological Systems XV (Vol. 11593, pp. 412-419). SPIE.
30. Doyle, J. F. (1989). Wave propagation in structures. Springer US.
31. Hwang, W., Bae, S., Kim, J., Kang, S., Kwag, N., & Lee, B. (2015). Acoustic emission characteristics of stress corrosion cracks in a type 304 stainless steel tube. Nuclear Engineering and Technology, 47(4), 454-460.
32. Vallen Systeme. AE-Sensor Data Sheet: VS150-WIC-V01. Available online: https://www.vallen.de/sensors/watertight-sensors/vs150-wic-v01-2/ (accessed on 8 May 2023).
33. ASTM E976-15; Standard Guide for Determining the Reproducibility of Acoustic Emission Sensor Response. American Society of Testing of Materials: West Conshohocken, PA, USA, 2015.
34. Kundu, T. (2014). Acoustic source localization. Ultrasonics, 54(1), 25-38.